LS-DYNA® Smoothed Particle Galerkin Method for Severe Deformation and Failure Analyses in Solids

C. T. Wu, Y. Guo and W. Hu

Livermore Software Technology Corporation

Outline

1. Methods in LS-DYNA for solids and structure analyses.
2. Numerical issues in conventional particle methods.
3. Smoothed particle Galerkin method for solid applications.
4. Benchmarks and numerical examples.
5. Keyword input format.
6. Conclusions and future plans.

LSTC Livermore Software Technology Corp.

Methods for Solid and Structural Analyses in LS-DYNA®

- *Rubber Materials*: FEM, EFG; MEFEM

- *Foam materials*: FEM, SPH, EFG, SPG

- *Metal materials*: FEM, SPH, EFG, MEFEM, Adaptive FEM and EFG

- *Quasi-brittle material fracture*: FEM, SPH, EFG, State-based Peridynamic method

- *E.O.S. materials and high speed applications*: ALE, SPH, SPG
State-based Peridynamic method

- *Shells*: FEM, EFG, SFEM
- *Soil*: ALE, SPH, EFG, SPG
- *Discrete materials*: discrete element method
- *Composites and Unit cell analysis*: FEM, EFG, Immersed Particle Galerkin method

Numerical Issues in Conventional Particle Analysis of Solids and Structures

- Lack of approximation consistency
  - → Impose first-order reproducing condition
- Tension instability
  - → Ensure material failure occurs before numerical fracture
- Material diffusion
  - → Use higher-order integration scheme
- Presence of spurious or zero-energy modes
  - → Need stabilization
- Difficulty in enforcing the boundary conditions
  - → Special treatments (Convex approximation…)

3D Smoothed Particle Galerkin Method

FEM

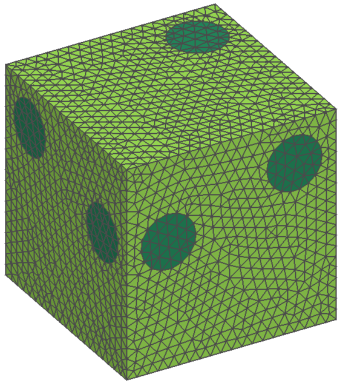

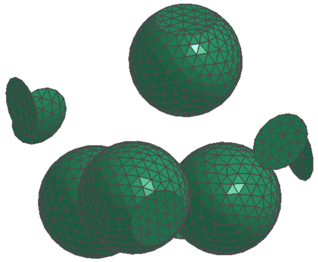

- Solid applications
- Read all FEM input formats
- A purely particle computation
- Handle severe deformation + failure

SPG

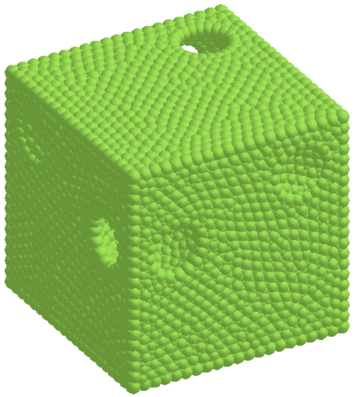

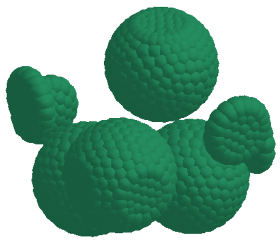

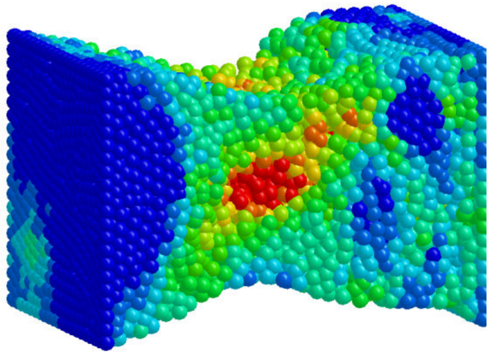

Main Features

Smoothed Particle Galerkin (SPG) Method

- Has explicit/implicit versions. Currently only explicit method implemented.
- A pure particle integration method without integration cell.
- Removes low-energy modes due to rank deficiency in nodal integration.
- Related to residual-based Galerkin meshfree method.
- Can be related to non-local or gradient types inelasticity.
- Without stabilization control parameters.
- Stability analysis via Variational Multi-scale analysis.
- First-order convergence in energy norm.
- Capable of providing a physical-based failure analysis.
- Has the trial version (will be formally released in this year).

Residual-based Meshfree Galerkin Principle

$$\bar{\boldsymbol{u}}(\boldsymbol{X}) \approx \int_\Omega \tilde{\Psi}(\boldsymbol{Y};\boldsymbol{X})\hat{\boldsymbol{u}}(\boldsymbol{X})d\Omega + \int_\Omega \tilde{\Psi}(\boldsymbol{Y};\boldsymbol{X})\nabla\hat{\boldsymbol{u}}(\boldsymbol{X})\cdot(\boldsymbol{Y}-\boldsymbol{X})d\Omega$$

$$+\frac{1}{2!}\int_\Omega \tilde{\Psi}(\boldsymbol{Y};\boldsymbol{X})\nabla^{(2)}\hat{\boldsymbol{u}}(\boldsymbol{X})\cdot^{(2)}(\boldsymbol{Y}-\boldsymbol{X})^{(2)}d\Omega$$

Displacement approximation

$$= \hat{\boldsymbol{u}}(\boldsymbol{X})\int_\Omega \tilde{\Psi}(\boldsymbol{Y};\boldsymbol{X})d\Omega + \nabla\hat{\boldsymbol{u}}(\boldsymbol{X})\left(\int_\Omega \tilde{\Psi}(\boldsymbol{Y};\boldsymbol{X})(\boldsymbol{Y})d\Omega - \boldsymbol{X}\int_\Omega \tilde{\Psi}(\boldsymbol{Y};\boldsymbol{X})d\Omega\right)$$

$$+\nabla^{(2)}\hat{\boldsymbol{u}}(\boldsymbol{X})\ \cdot^{(2)}\left(\frac{1}{2!}\int_\Omega \tilde{\Psi}(\boldsymbol{Y};\boldsymbol{X})(\boldsymbol{Y}-\boldsymbol{X})^{(2)}d\Omega\right)$$

$$= \hat{\boldsymbol{u}}(\boldsymbol{X})\int_\Omega \tilde{\Psi}(\boldsymbol{Y};\boldsymbol{X})d\Omega + \nabla^{(2)}\hat{\boldsymbol{u}}(\boldsymbol{X})\cdot^{(2)}\left(\frac{1}{2!}\int_\Omega \tilde{\Psi}(\boldsymbol{Y};\boldsymbol{X})(\boldsymbol{Y}-\boldsymbol{X})^{(2)}d\Omega\right)$$

$$= \hat{\boldsymbol{u}}(\boldsymbol{X}) + \nabla^{(2)}\hat{\boldsymbol{u}}(\boldsymbol{X})\cdot^{(2)}\boldsymbol{\eta}(\boldsymbol{X}) \Longrightarrow$$

Gradient type nonlocal strain

Variational formulation

$\Longrightarrow$

$$a^h(\hat{\boldsymbol{u}},\delta\hat{\boldsymbol{u}}) = l(\delta\hat{\boldsymbol{u}})\ \forall\delta\hat{\boldsymbol{u}}\in\boldsymbol{V}^h$$

$$a^h(\hat{\boldsymbol{u}},\delta\hat{\boldsymbol{u}}) = \int_\Omega \delta(\nabla^s\hat{\boldsymbol{u}}):\boldsymbol{C}:(\nabla^s\hat{\boldsymbol{u}})d\Omega + \int_\Omega \delta\left(\overline{\nabla}^{(2)}\hat{\boldsymbol{u}}\right):\boldsymbol{C}:\left(\overline{\nabla}^{(2)}\hat{\boldsymbol{u}}\right)d\Omega$$

$$= a^h_{stan}(\hat{\boldsymbol{u}},\delta\hat{\boldsymbol{u}}) + a^h_{stab}(\hat{\boldsymbol{u}},\delta\hat{\boldsymbol{u}})$$

$$a^h_{stab}(\hat{\boldsymbol{u}},\delta\hat{\boldsymbol{u}}) = \int_\Omega \delta\left(\overline{\nabla}^{(2)}\hat{\boldsymbol{u}}\right):\boldsymbol{C}:\left(\overline{\nabla}^{(2)}\hat{\boldsymbol{u}}\right)d\Omega$$

$$\overline{\nabla}^{(2)}\hat{\boldsymbol{u}} = \frac{1}{2}\left(\nabla\boldsymbol{\eta}:\hat{\boldsymbol{u}}\nabla^{(2)} + \nabla^{(2)}\hat{\boldsymbol{u}}:\boldsymbol{\eta}\nabla\right)$$

$$l(\delta\hat{\boldsymbol{u}}) = \int_\Omega \delta\hat{\boldsymbol{u}}\cdot\boldsymbol{f}d\Omega + \int_{\Gamma_N}\delta\hat{\boldsymbol{u}}\cdot\boldsymbol{t}d\Gamma - \int_\Omega\left(\delta\nabla^{(2)}\hat{\boldsymbol{u}}:\boldsymbol{\eta}\right)\cdot\boldsymbol{f}d\Omega$$

Wu *et. al* submitted to J. Comput. Physics. (2014)

Well-defined Mathematical Property

Coercivity

$$\|\hat{\boldsymbol{u}}\|_1^2 \le c_1 \|\nabla^s \hat{\boldsymbol{u}}\|_0^2 \le c_1 \left(\|\nabla^s \hat{\boldsymbol{u}}\|_0^2 + \left\|\overline{\nabla}^{(2)} \hat{\boldsymbol{u}}\right\|_0^2 \right)$$

$$\le \frac{c_1}{\gamma_{\min}(\boldsymbol{C})} \left(a_{stan}^h(\hat{\boldsymbol{u}},\hat{\boldsymbol{u}}) + a_{stab}^h(\hat{\boldsymbol{u}},\hat{\boldsymbol{u}}) \right)$$

$$= c_2 a^h(\hat{\boldsymbol{u}},\hat{\boldsymbol{u}}),\ c_1, c_2 > 0,\ \hat{\boldsymbol{u}} \in \boldsymbol{V}^h$$

Continuity

$$\left| a^h(\hat{\boldsymbol{u}},\hat{\boldsymbol{v}}) \right| \le \int_\Omega \left| (\nabla^s \hat{\boldsymbol{u}}) : \boldsymbol{C} : (\nabla^s \hat{\boldsymbol{v}}) \right| d\Omega + \int_\Omega \left| \left(\overline{\nabla}^{(2)} \hat{\boldsymbol{u}}\right) : \boldsymbol{C} : \left(\overline{\nabla}^{(2)} \hat{\boldsymbol{v}}\right) \right| d\Omega$$

$$\le \gamma_{\max}(\boldsymbol{C}) \left\{ \left(\int_\Omega \|\hat{\boldsymbol{\varepsilon}}(\hat{\boldsymbol{u}})\|_0^2 d\Omega \right)^{1/2} + \left(\int_\Omega \|\hat{\boldsymbol{\varepsilon}}(\hat{\boldsymbol{v}})\|_0^2 d\Omega \right)^{1/2} \right.$$

$$\left. +\ c_3 \left(\int_\Omega \|h \nabla \hat{\boldsymbol{\varepsilon}}(\hat{\boldsymbol{u}})\|_0^2 d\Omega \right)^{1/2} + \left(\int_\Omega \|h \nabla \hat{\boldsymbol{\varepsilon}}(\hat{\boldsymbol{v}})\|_0^2 d\Omega \right)^{1/2} \right\}$$

$$\le \gamma_{\max}(\boldsymbol{C}) c_4 \left\{ |\hat{\boldsymbol{u}}|_1 |\hat{\boldsymbol{v}}|_1 \right\} \quad \le c_5 \|\hat{\boldsymbol{u}}\|_1 \|\hat{\boldsymbol{v}}\|_1,\quad c_3, c_4, c_5 > 0 \quad \forall \hat{\boldsymbol{u}},\ \hat{\boldsymbol{v}} \in \boldsymbol{V}^h$$

$+$ … $=$ *Unique solution !*

Error Estimation via Variational Multi-scale Method

$$\begin{cases} a^h(\boldsymbol{v}^h, \boldsymbol{u}^h) + a^h(\boldsymbol{v}^h, \boldsymbol{u}^b) = l(\boldsymbol{v}^h) \ \forall \boldsymbol{v}^h \in \boldsymbol{V}^h \\ a^h(\boldsymbol{v}^b, \boldsymbol{u}^h) + a^h(\boldsymbol{v}^b, \boldsymbol{u}^b) = l(\boldsymbol{v}^b) \ \forall \boldsymbol{v}^b \in \boldsymbol{B}^h \end{cases}$$

coarse-scale equation

fine-scale equation

$$\boldsymbol{B}^h(\Omega) := \{\boldsymbol{v}^b : \boldsymbol{v}^b \in \boldsymbol{H}^1, \boldsymbol{v}^b = \boldsymbol{0} \ on\, \Gamma\}$$

global residual-free fine-scale space

$$\bar{\boldsymbol{u}}^h(\boldsymbol{x}) = \sum_{J=1}^{NP} \tilde{\Psi}_J(\boldsymbol{x}) \hat{\boldsymbol{u}}_J$$

$$= \sum_{J=1}^{NP} \tilde{\Psi}_J(\boldsymbol{x}) \sum_{K=1}^{NP} \Psi_K(\boldsymbol{x}_J) \tilde{\boldsymbol{u}}_K$$

$$\Longrightarrow \quad = \sum_{K=1}^{NP} \sum_{J=1}^{NP} \Psi_K(\boldsymbol{x}_J) \tilde{\Psi}_J(\boldsymbol{x}) \tilde{\boldsymbol{u}}_K \quad \Longrightarrow \quad \boldsymbol{u}^b \approx \left(\sum_{I=1}^{BP} (\phi_I(\boldsymbol{x}) - \Psi_I(\boldsymbol{x})) \tilde{\boldsymbol{u}}_I^b(\boldsymbol{x}_I) \right) = \sum_{I=1}^{BP} \Psi_I^b(\boldsymbol{x}) \tilde{\boldsymbol{u}}_I^b(\boldsymbol{x}_I), \forall \boldsymbol{x}_I \in Z_I^b$$

fine-scale approximation

$$= \sum_{K=1}^{NP} \phi_K(\boldsymbol{x}) \tilde{\boldsymbol{u}}_K$$

$$\Longrightarrow \quad \bar{\boldsymbol{u}}^h = \boldsymbol{u}^h + \boldsymbol{u}^b = \boldsymbol{\Psi}^T \boldsymbol{K}^{-1} \left(-\boldsymbol{K}^{b^T} \tilde{\boldsymbol{K}}^{-1} \tilde{\tilde{\boldsymbol{R}}} + \boldsymbol{R} \right) + \boldsymbol{\Psi}^{b^T} \tilde{\boldsymbol{K}}^{-1} \tilde{\boldsymbol{R}}$$

$$\Longrightarrow \quad \bar{a}^h(\boldsymbol{u}-\boldsymbol{u}^h, \boldsymbol{u}-\boldsymbol{u}^h) = a^h(\boldsymbol{u}-\boldsymbol{u}^h, \boldsymbol{u}-\boldsymbol{u}^h) + a^{\boldsymbol{h}}_{stab}(\boldsymbol{u}-\boldsymbol{u}^h, \boldsymbol{u}-\boldsymbol{u}^h)$$

$$\leq \left\| \boldsymbol{u}-\boldsymbol{u}^h \right\|_e^2 + h^2 \left\| \Delta(\boldsymbol{u}-\boldsymbol{u}^h) \right\|_e^2$$

Error estimation in energy-norm

$$\leq c_{(\mu,\lambda)} h^2 |\boldsymbol{u}|_{2,\Omega}^2 + \tilde{c}_{(\mu,\lambda)} h^2 |\boldsymbol{u}|_{2,\Omega}^2 \leq \bar{c}_{(\mu,\lambda)} h^2 |\boldsymbol{u}|_{2,\Omega}^2$$

Nonlinear SPG Implementation

Implicit formulation

$$\Delta\delta\Pi = \int_{\Omega_x} \delta\varepsilon_{ij} C_{ijkl} \Delta\varepsilon_{kl} d\Omega + \int_{\Omega_x} \delta u_{i,j} T_{ijkl} \Delta u_{k,l} d\Omega - \int_{\Omega_x} \delta u_i \Delta f_i d\Omega - \int_{\Gamma_N} \delta u_i \Delta t_i d\Gamma$$

$\Longrightarrow$ $$\delta\tilde{\boldsymbol{U}}^T \boldsymbol{K}_{n+1}^{v} \left(\Delta\tilde{\boldsymbol{U}}\right)_{n+1}^{v+1} = \delta\tilde{\boldsymbol{U}}^T \boldsymbol{R}_{n+1}^{v}$$

$\Longrightarrow$ $$\tilde{\boldsymbol{U}} = \boldsymbol{A}^{-1}\overline{\boldsymbol{U}}$$

$$\boldsymbol{A}_{IJ} = \phi_J(\boldsymbol{X}_I)\boldsymbol{I} = \sum_{K=1}^{NP} \Psi_K(\boldsymbol{X}_I)\Psi_J(\boldsymbol{X}_K)\boldsymbol{I}$$

$$\boldsymbol{A}^{-T} \boldsymbol{K}_{n+1}^{v} \boldsymbol{A}^{-1} \left(\Delta\overline{\boldsymbol{U}}\right)_{n+1}^{v+1} = \boldsymbol{A}^{-T} \boldsymbol{R}_{n+1}^{v}$$

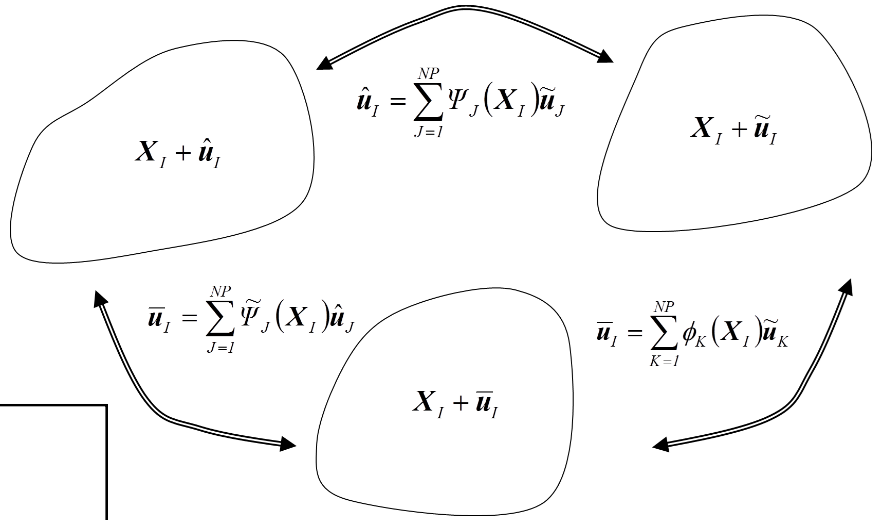

Corresponding coordinate systems in SPG computation

Explicit dynamic formulation

$\Longrightarrow$ $$\boldsymbol{A}^{-T} \boldsymbol{M} \boldsymbol{A}^{-1} \ddot{\overline{\boldsymbol{U}}} = \boldsymbol{A}^{-T}\left(\boldsymbol{f}^{ext} - \boldsymbol{f}^{\text{int}}\right)$$

$\Longrightarrow$ $$\overline{\boldsymbol{M}}\ddot{\overline{\boldsymbol{U}}} = \boldsymbol{A}^{-T}\left(\boldsymbol{f}^{ext} - \boldsymbol{f}^{\text{int}}\right)$$

$$\overline{\boldsymbol{M}}_I^{RS} = \sum_J^{NP} \overline{\boldsymbol{M}}_{IJ} = \sum_J^{NP} \boldsymbol{A}_{IK}^{-T} \boldsymbol{M}_{KM} \boldsymbol{A}_{ML}^{-1}$$

$$\frac{d\rho_I}{dt} = -\rho_I \nabla \cdot \left(\dot{\tilde{\boldsymbol{u}}}_I\right) = -\rho_I \sum_{J=1}^{NP} \dot{\tilde{\boldsymbol{u}}}_J \cdot \Psi_{J,\boldsymbol{x}}(\boldsymbol{x}_I)$$

Currently implemented in LS-DYNA©

Updated Lagrangain /Eulerian Kernels

$$\Psi^{-}_{I,i}\left(\boldsymbol{x}^{k+1}\right)=\frac{\partial \Psi^{-}_{I}\left(\boldsymbol{x}^{k+1}\right)}{\partial x_i^{k+1}}=\frac{\partial \Psi^{-}_{I}\left(\boldsymbol{x}^{k+1}\right)}{\partial x_j^{k}}\frac{\partial x_j^{k}}{\partial x_j^{k+1}}=\frac{\partial \Psi^{-}_{I}}{\partial x_j^{k}}f_{ji}^{k-1}$$

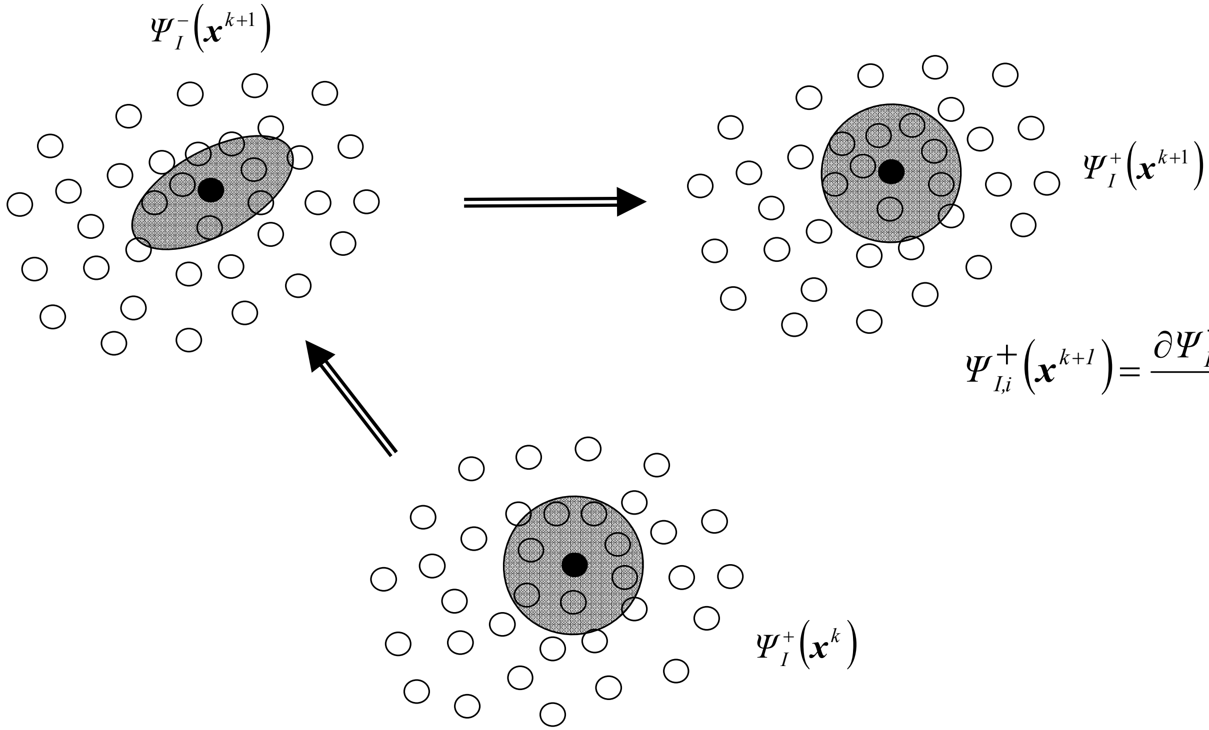

$$\Psi^{+}_{I,i}\left(\boldsymbol{x}^{k+1}\right)=\frac{\partial \Psi^{+}_{I}\left(\boldsymbol{x}^{k+1}\right)}{\partial x_i}$$

Consistency + Stability = Convergence

First-order rate of convergence in energy norm !

Material fracture v.s. Numerical fracture

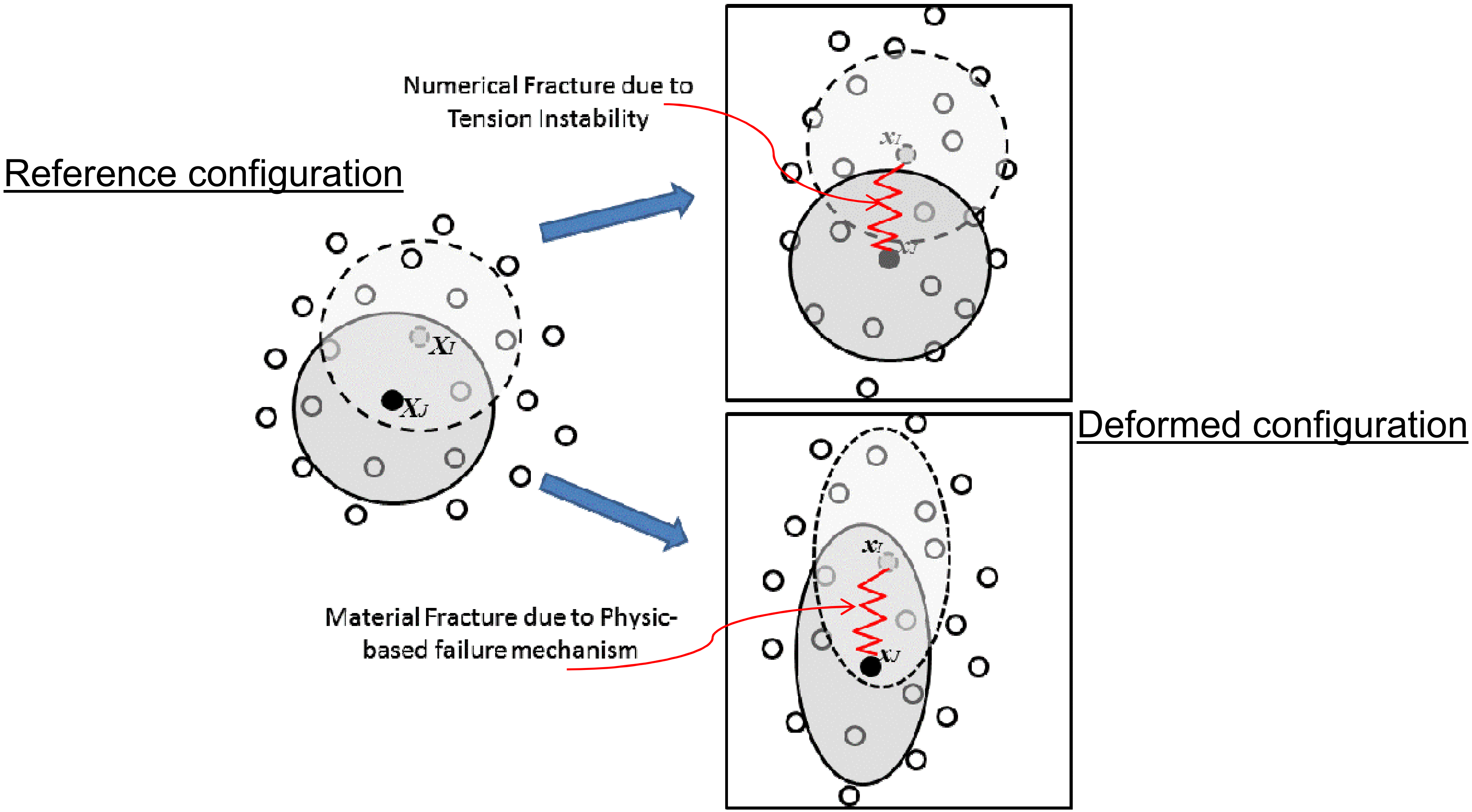

physical material fracture before numerical fracture ⟶ ***Enlarge numerical support !***

Prandtl's punch problem

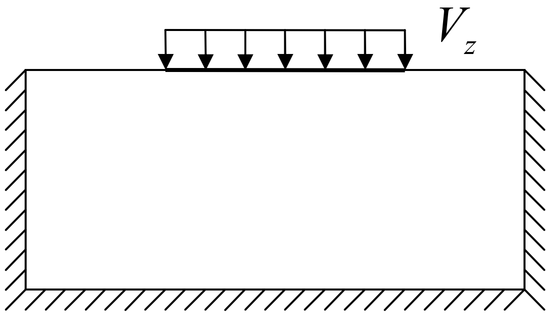

Dimension: 4x2x1

Particles: 21x11x6

Elastic material: $E=6.9\text{x}10^4$

$v=0.3$

$V_z=2$

$\rho_0=2.7\times10^3$

Updated Lagrangian

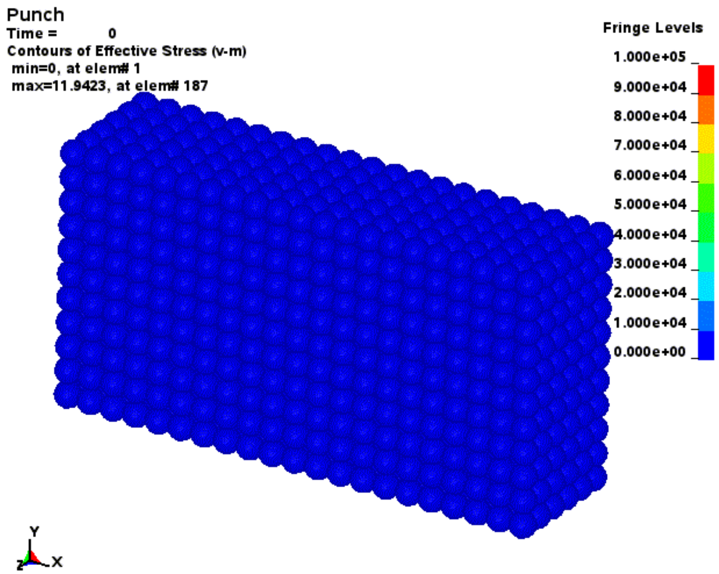

Eulerian

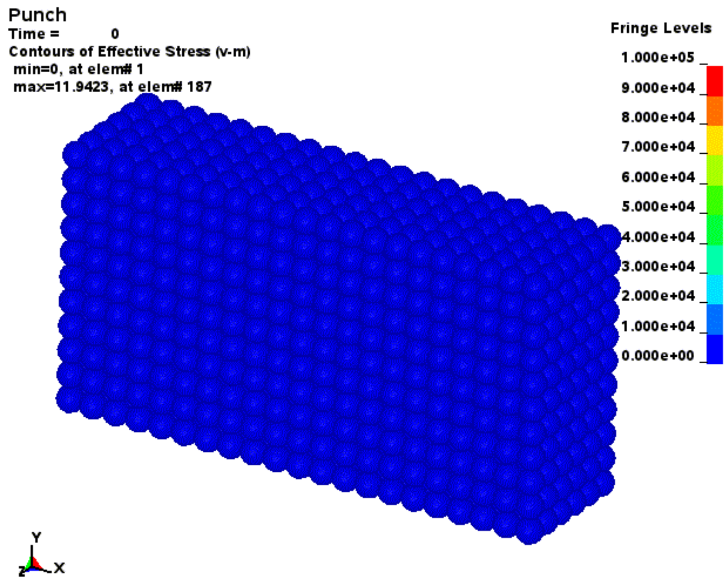

Prandtl's punch problem

Updated Lagrangian

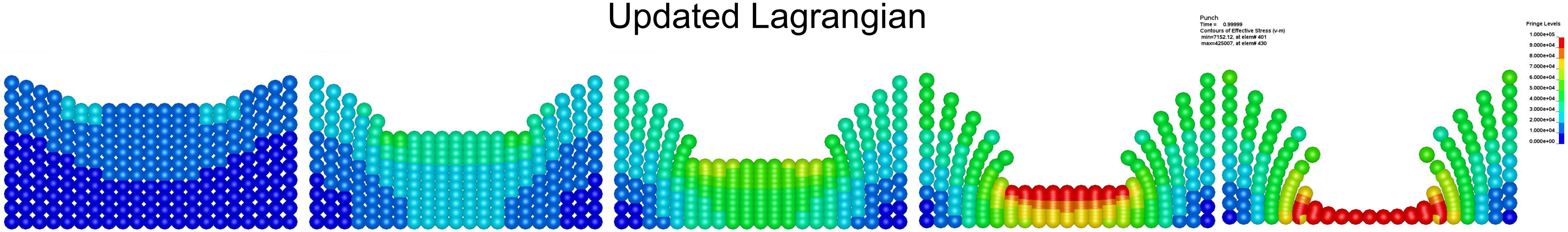

Fixed $\Delta t=3.0\times10^{-5}$

t=0.2 0.4 0.6 0.8 1.0

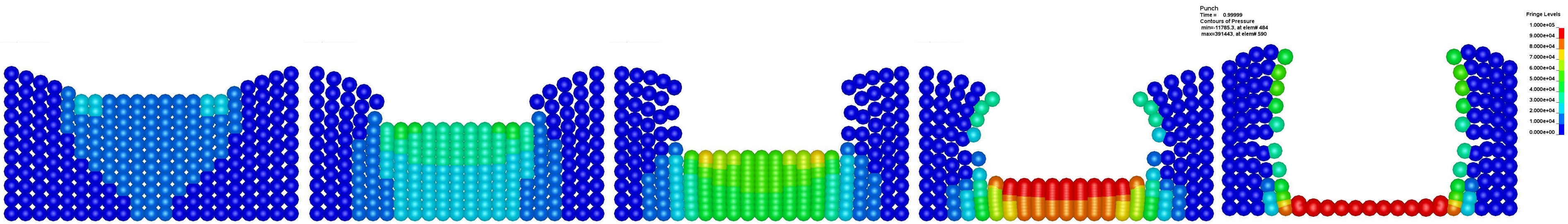

Eulerian

Prandtl's punch problem

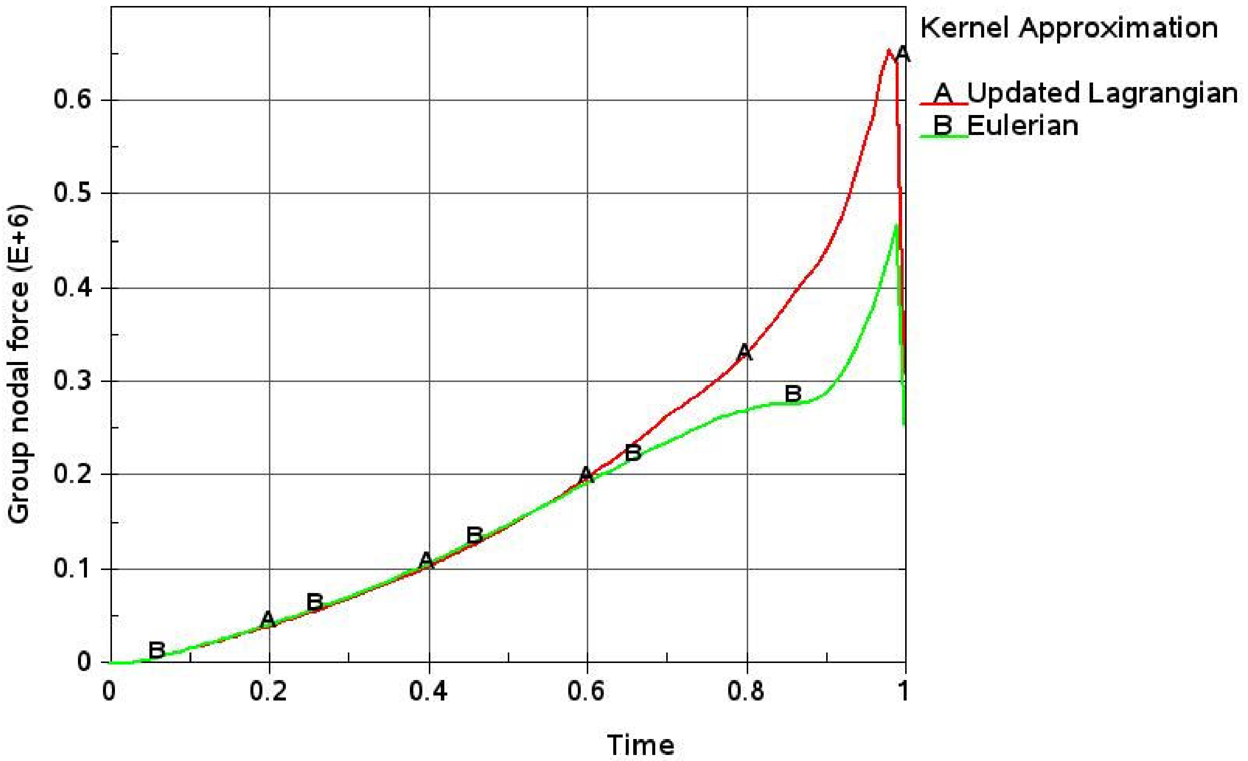

Nodal force comparison with different kernel approximations

Taylor Bar Impact

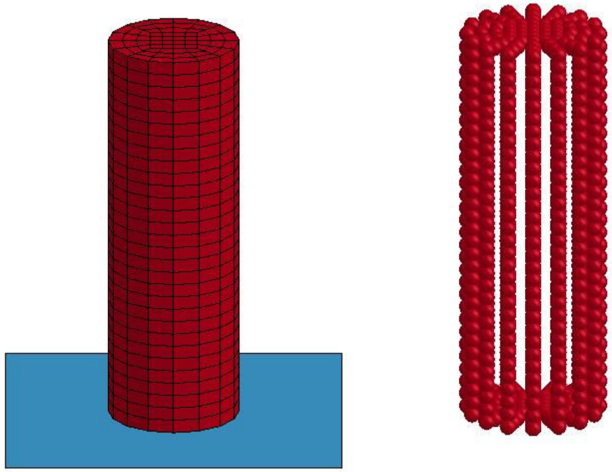

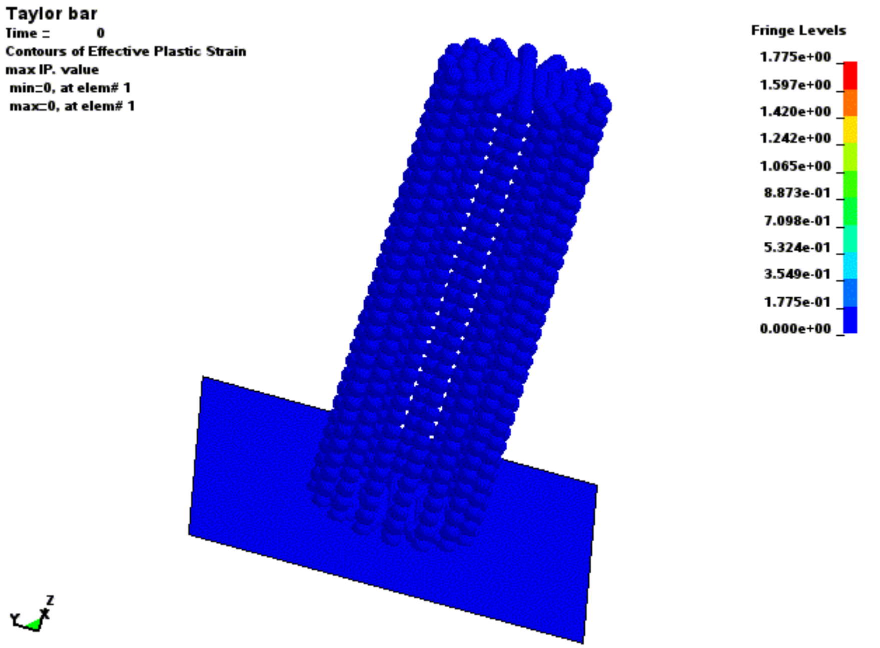

R=3.91 mm
H=23.46 mm
$\rho_0=2.7\times10^{-6}$ kg/mm^3
E=78.2GPa
v=0.3
$\sigma_y=0.29(1+125e^p)^{0.1}$
V_0=373 mm/ms

Particles: 2263
DX=DY=DZ=1.4   SMSTEP=25

Final H=18.07mm

Exp. H=16.51mm

Taylor Bar Impact

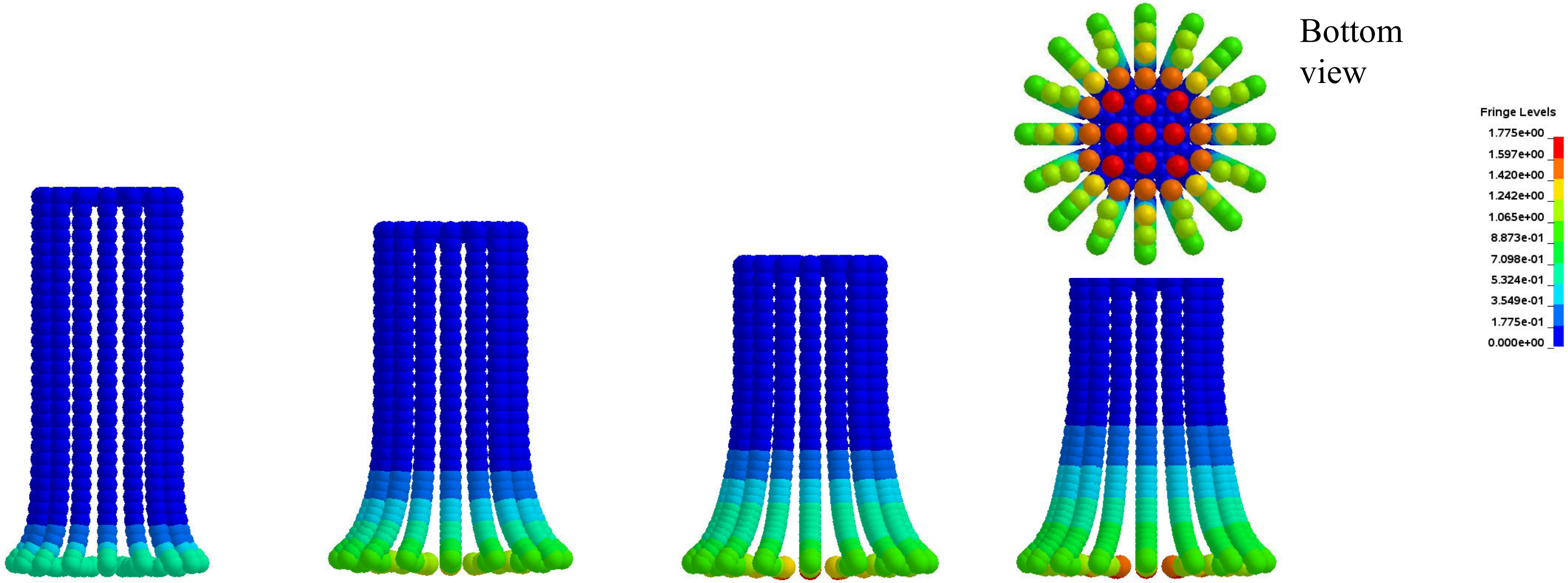

t=0.004	0.012	0.020	0.028
$\Delta t=1.76\times10^{-5}$	1.72×10^{-5}	1.66×10^{-5}	1.66×10^{-5}

Progressive deformation with effective plastic strain contour

Plate Impact (Ductile Material)

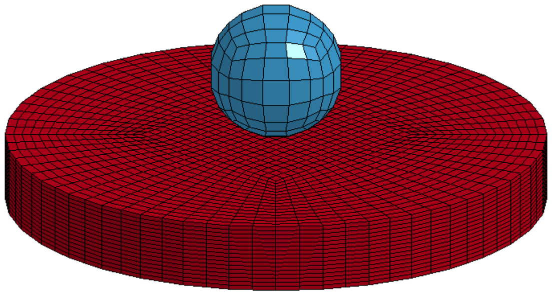

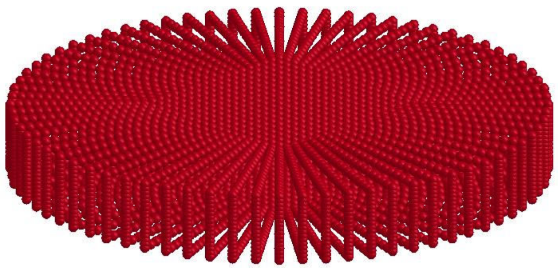

Ball: rigid, R=5.0

Plate: R=20.0, thickness=5.0

Particles: 25721, updated Lagrangian

Elastic perfectly-plastic material:

$\rho_0 = 7.85 \times 10^{-3}$

$E = 6.9 \times 10^4$

$\nu = 0.3$

$\sigma_y = 200.0$

$V_z = -600.0, -400.0, -300.0$

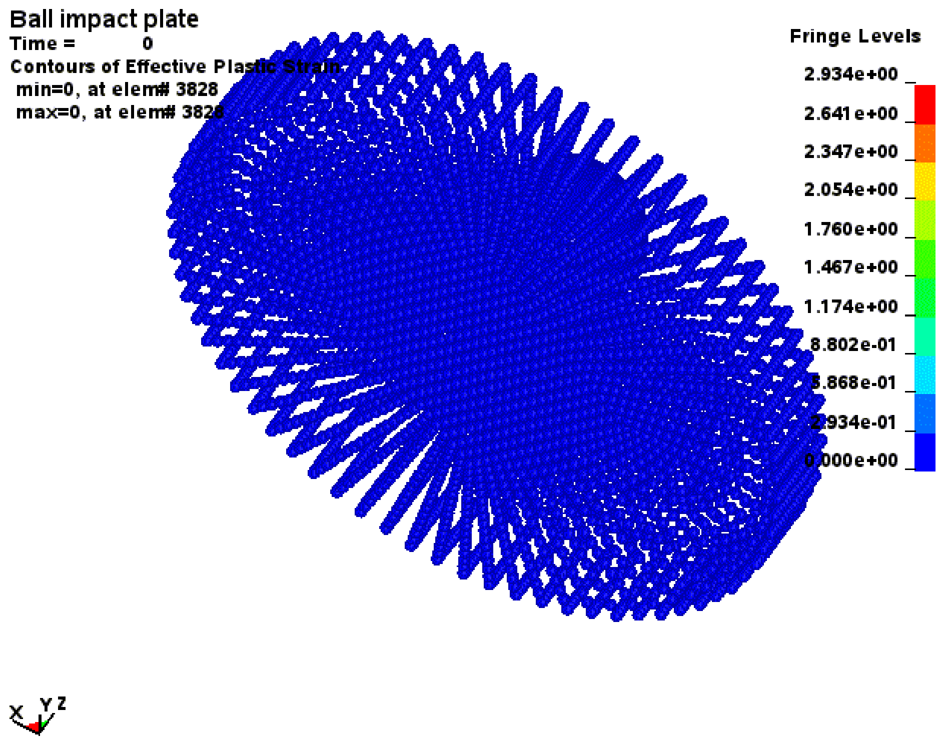

Plate Impact

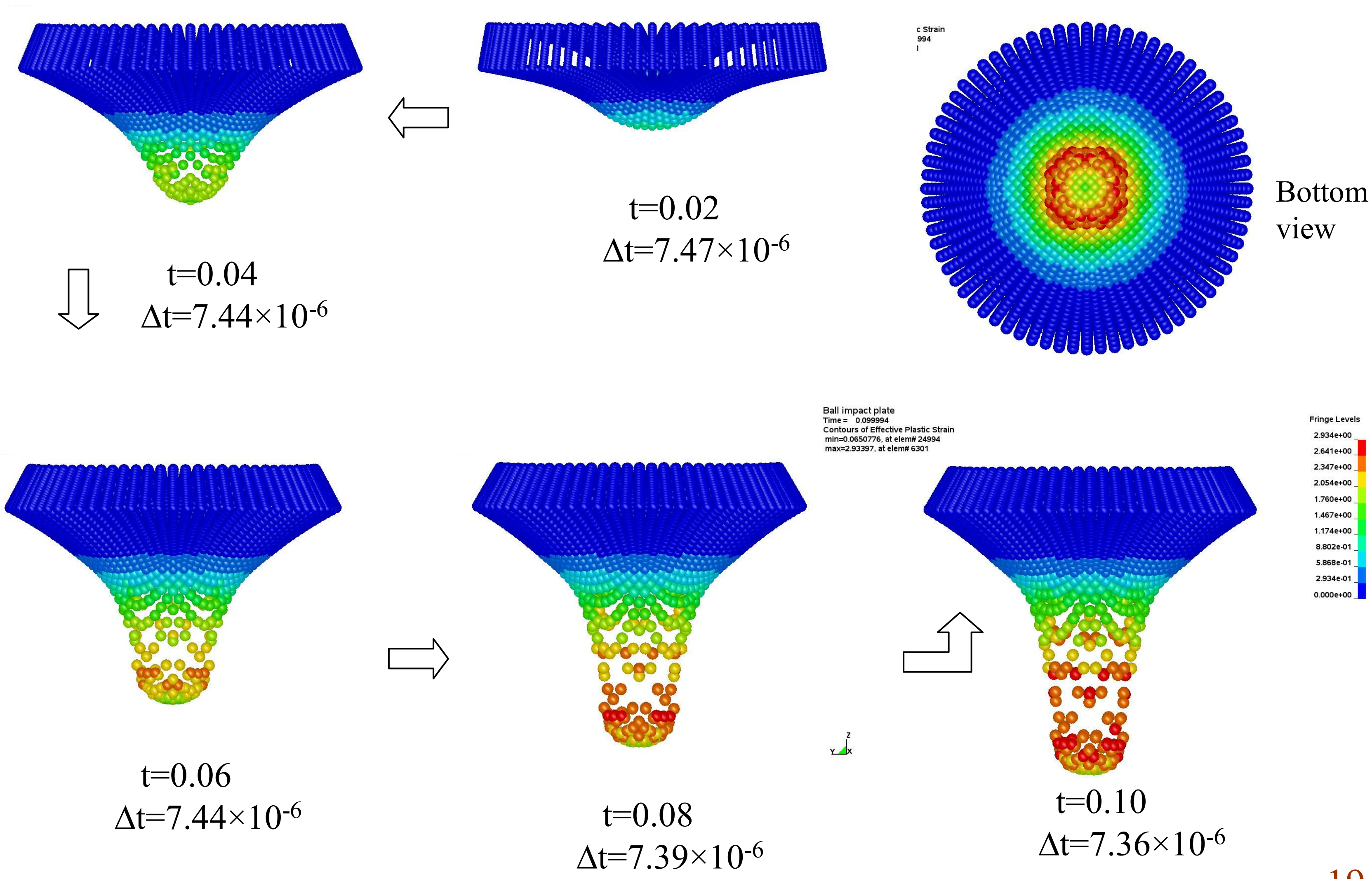

Effective plastic strain (v=600, t=0.06)

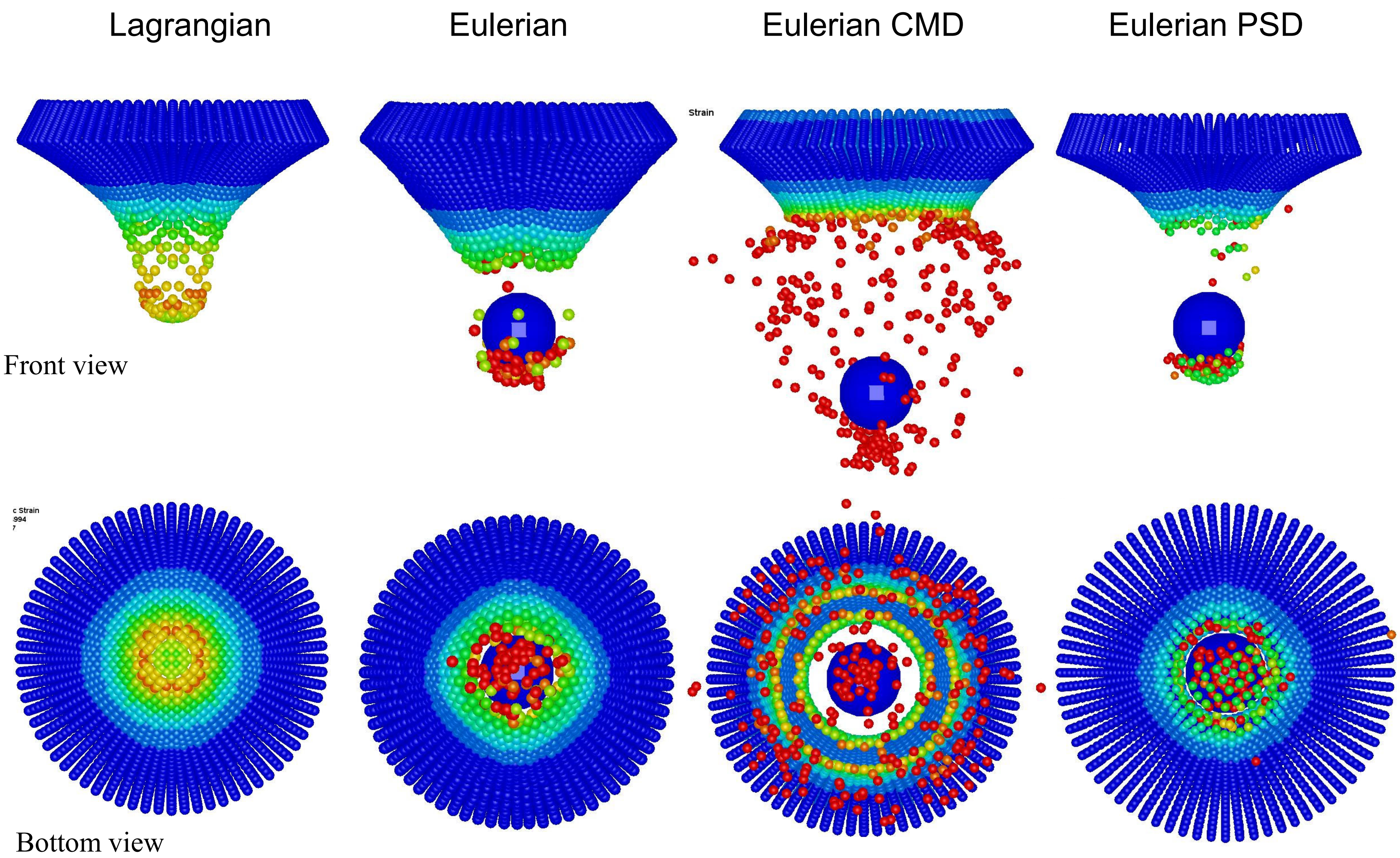

Progressive effective plastic strain plots with phenomenological strain-based damage (v=400)

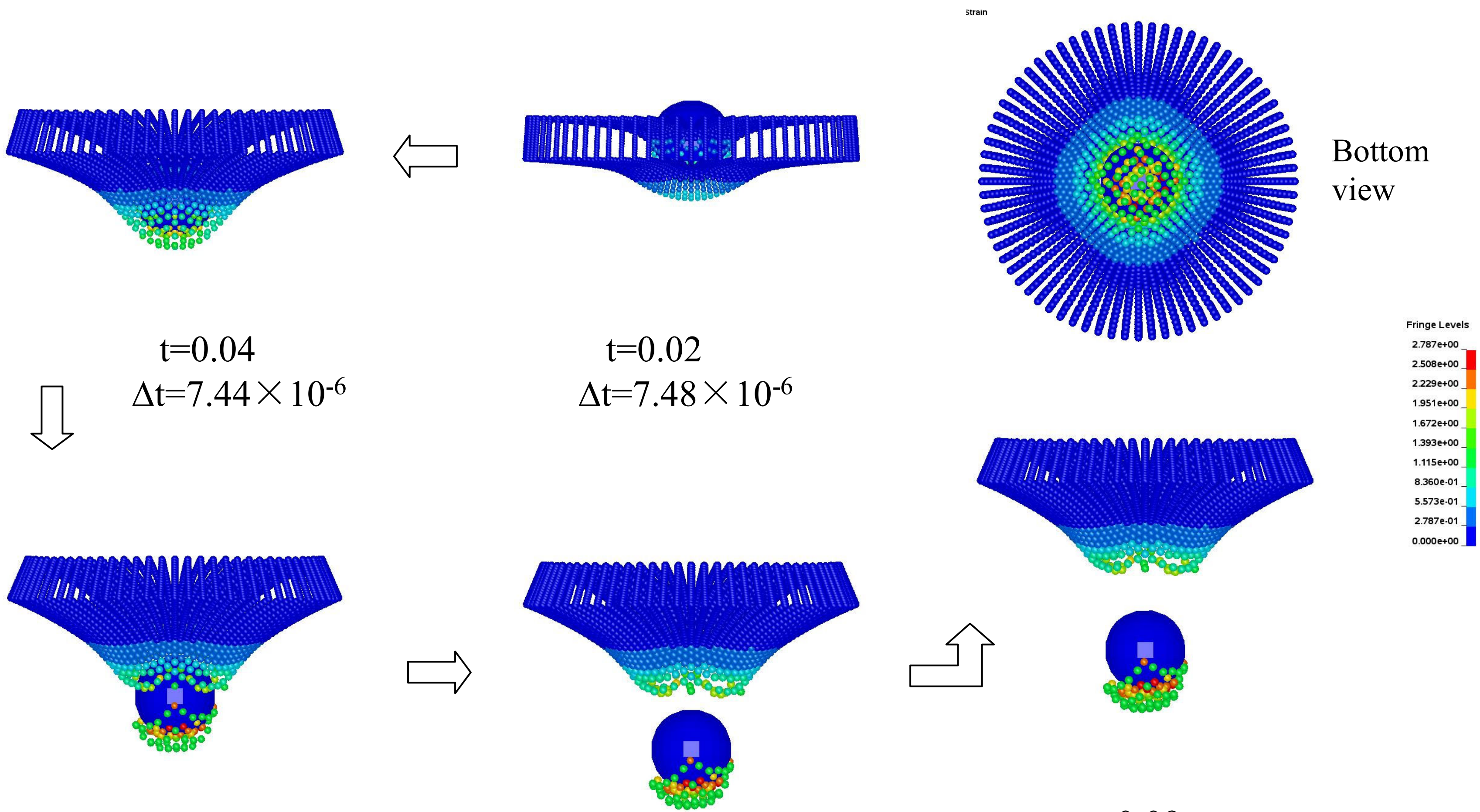

t=0.02 $\Delta t=7.48\times10^{-6}$

t=0.04 $\Delta t=7.44\times10^{-6}$

t=0.06 $\Delta t=7.47\times10^{-6}$

t=0.08 $\Delta t=7.48\times10^{-6}$

t=0.09 $\Delta t=7.44\times10^{-6}$

Effective plastic strain with phenomenological strain-based damage

v=300
t=0.12

v=400
t=0.09

v=600
t=0.06

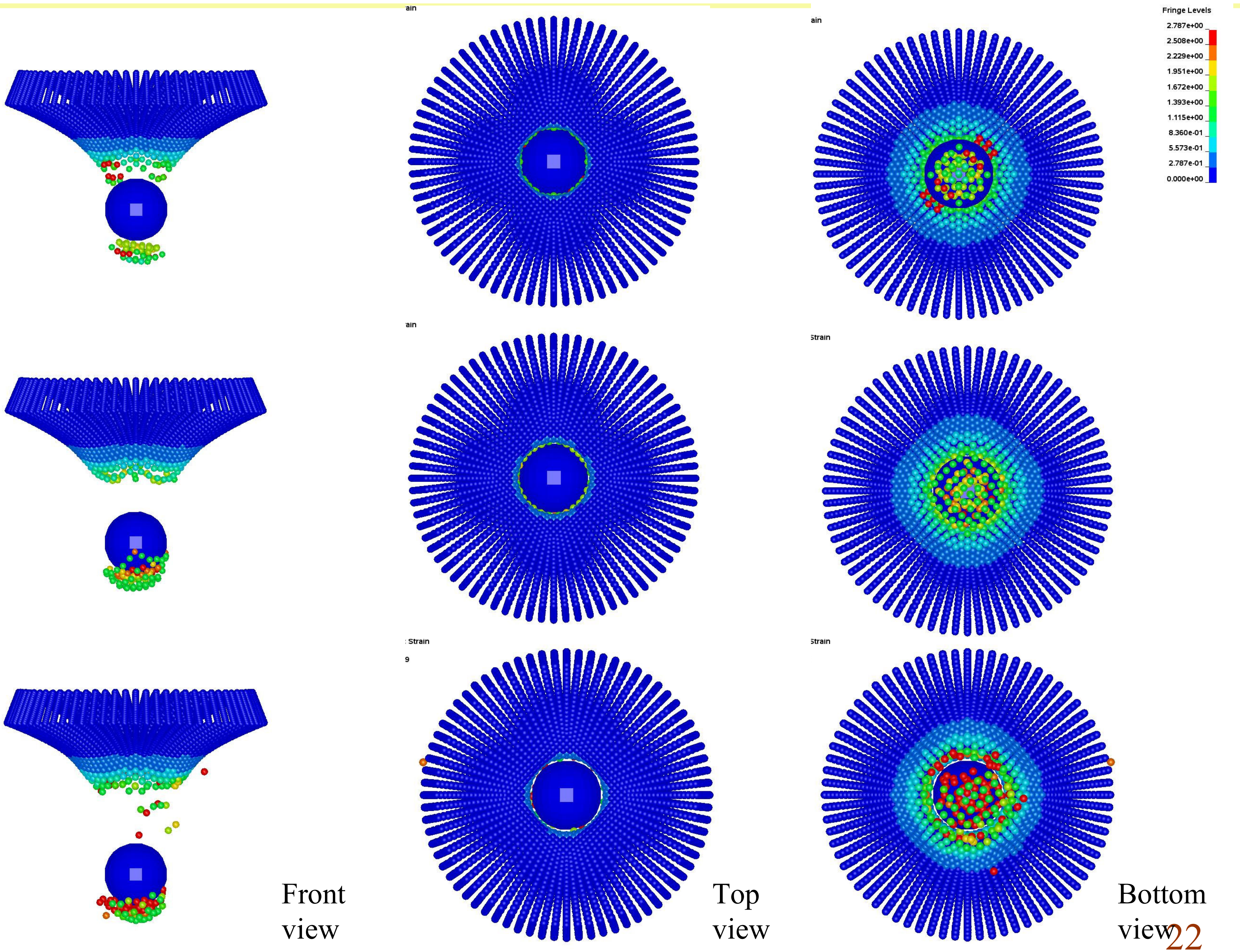

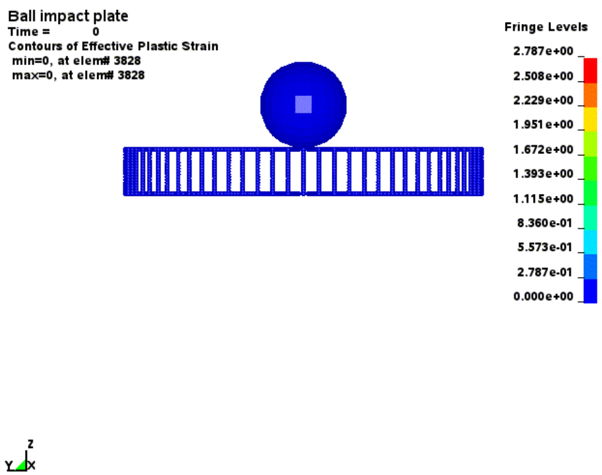

v=300

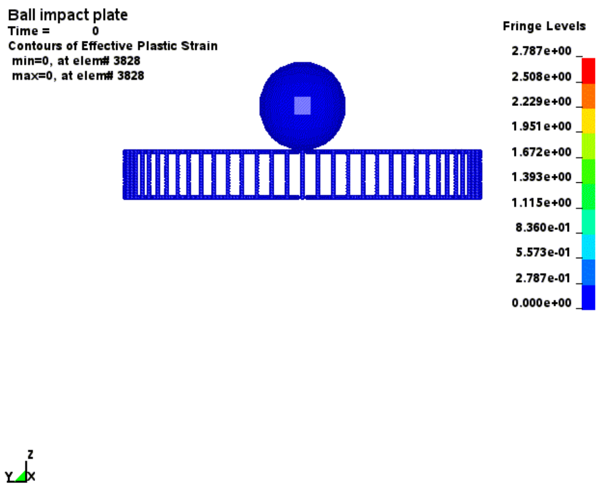

v=400

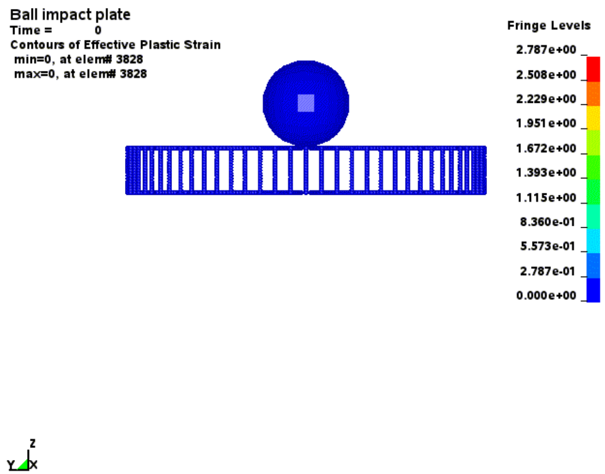

v=600

Plate Impact (Brittle Material)

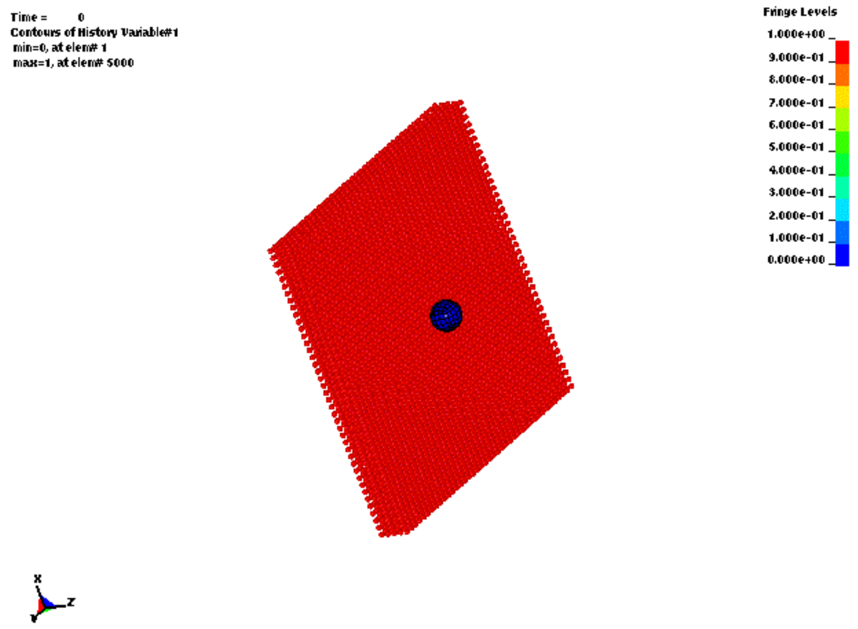

Damage Indicator
(movie)

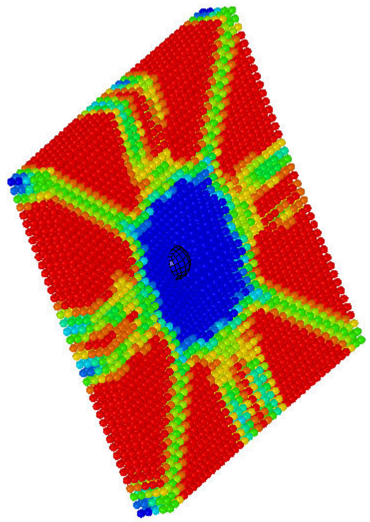

Front View

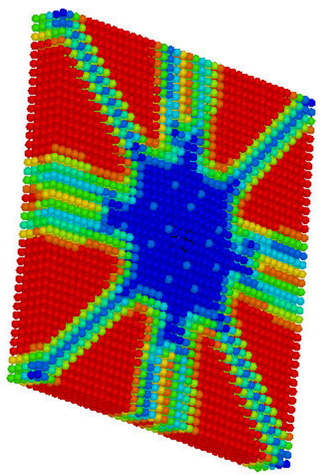

Back View

Final Crack Pattern

Metal cutting analysis (1)

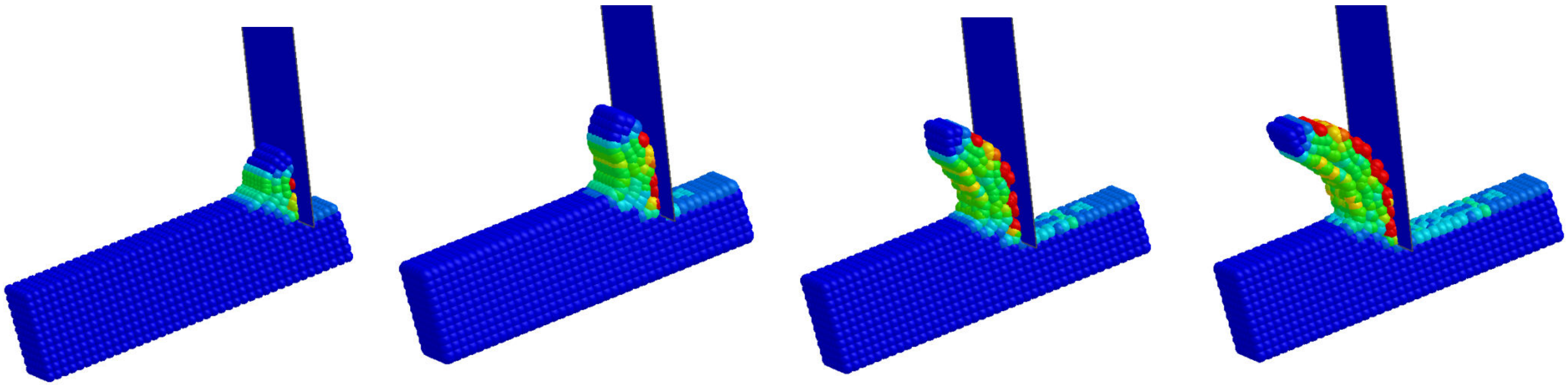

Aluminum
$\rho_0 = 2.7 \times 10^{-6}$ kg/mm^3
E=78.2GPa
v=0.3
$\sigma_y = 0.29(1+125e^p)^{0.1}$

Strain-based failure criteria $\varepsilon^{fail} = 0.5$

Cutting Speed = 10 m/s
Fixed $\Delta t = 3.0 \times 10^{-5}$

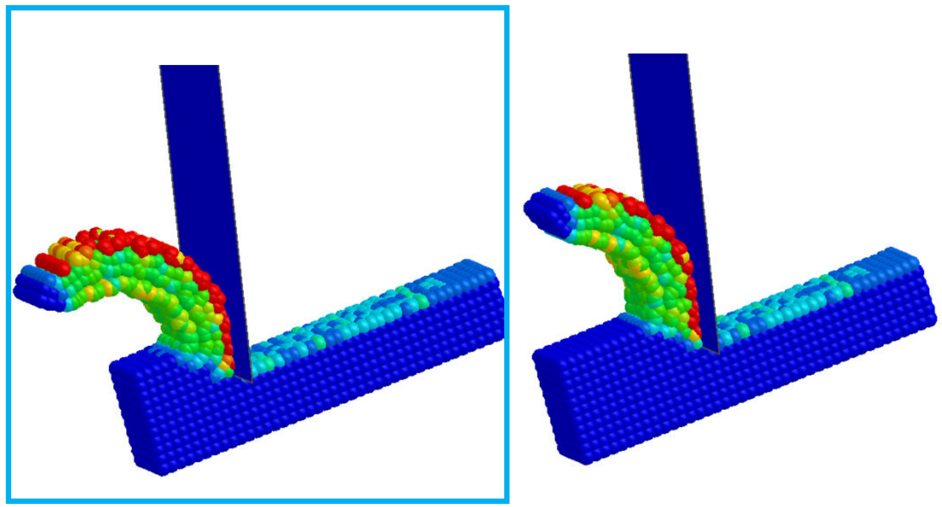

Metal cutting analysis (2)

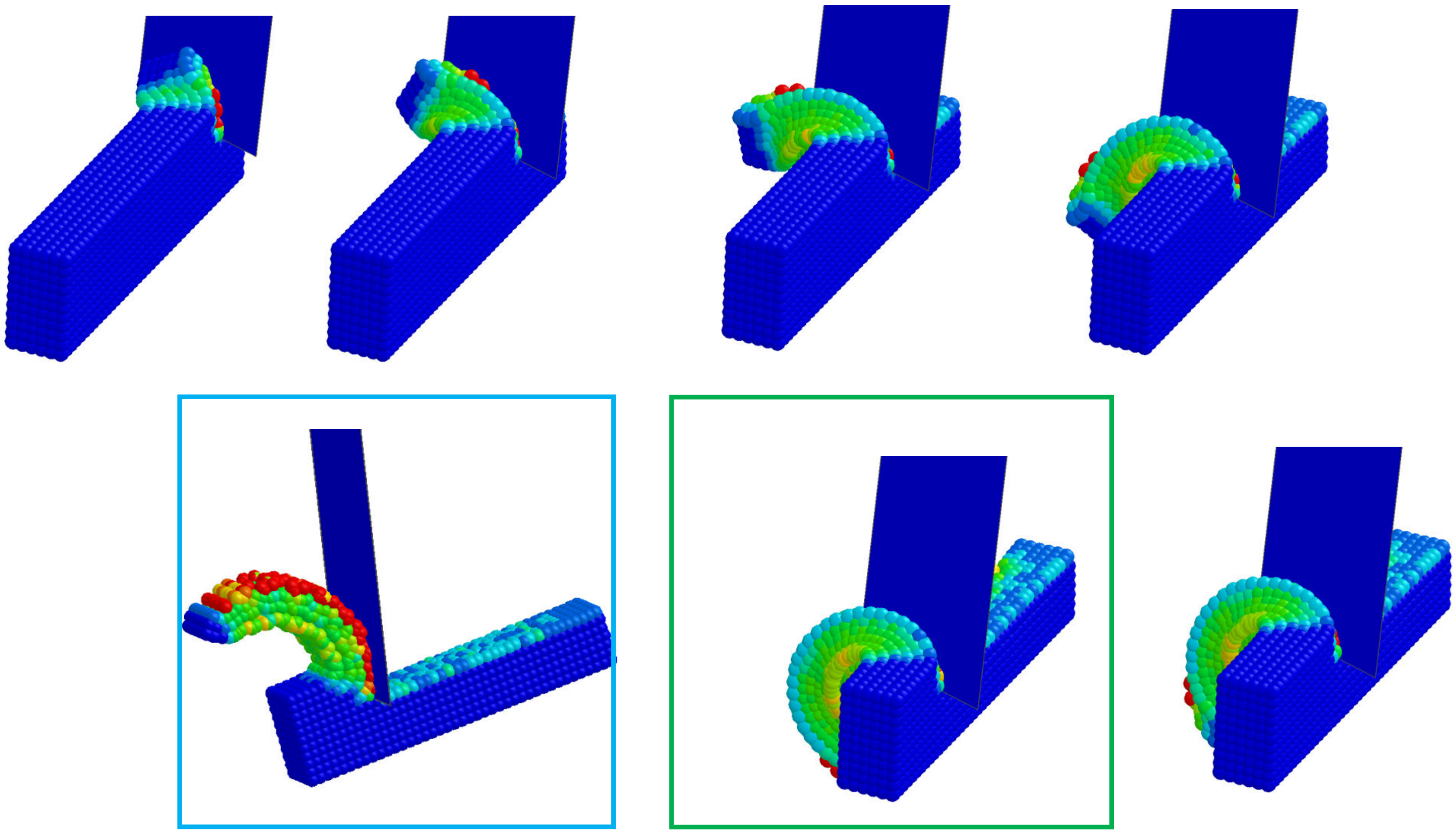

Cutting Speed = 10 m/s
with different cutting angle

Fixed $\Delta t = 3.0 \times 10^{-5}$

Metal cutting analysis (3)

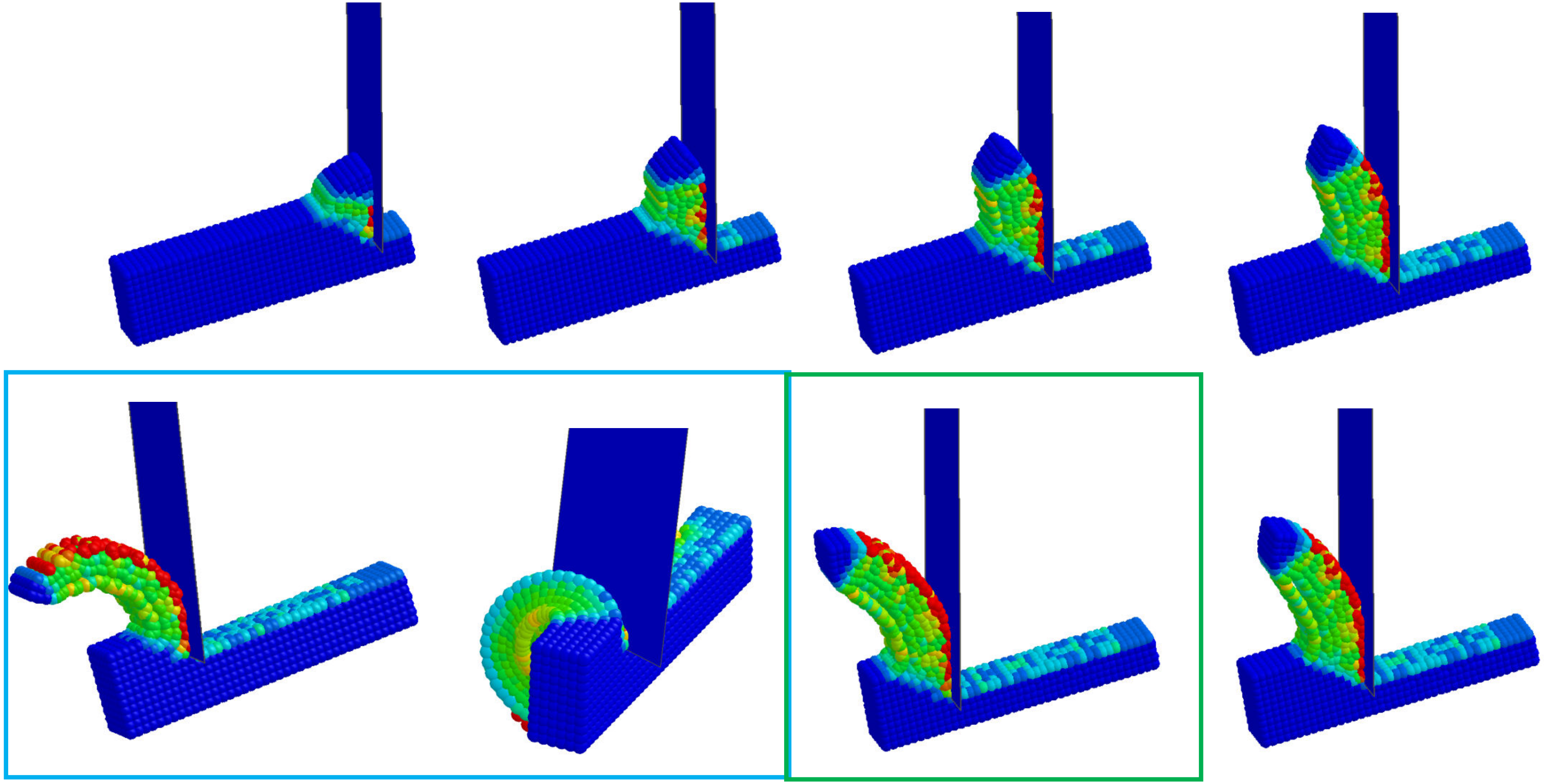

Cutting Speed = 10 m/s
with different depth

Fixed $\Delta t=3.0\times10^{-5}$

Metal cutting analysis (4)

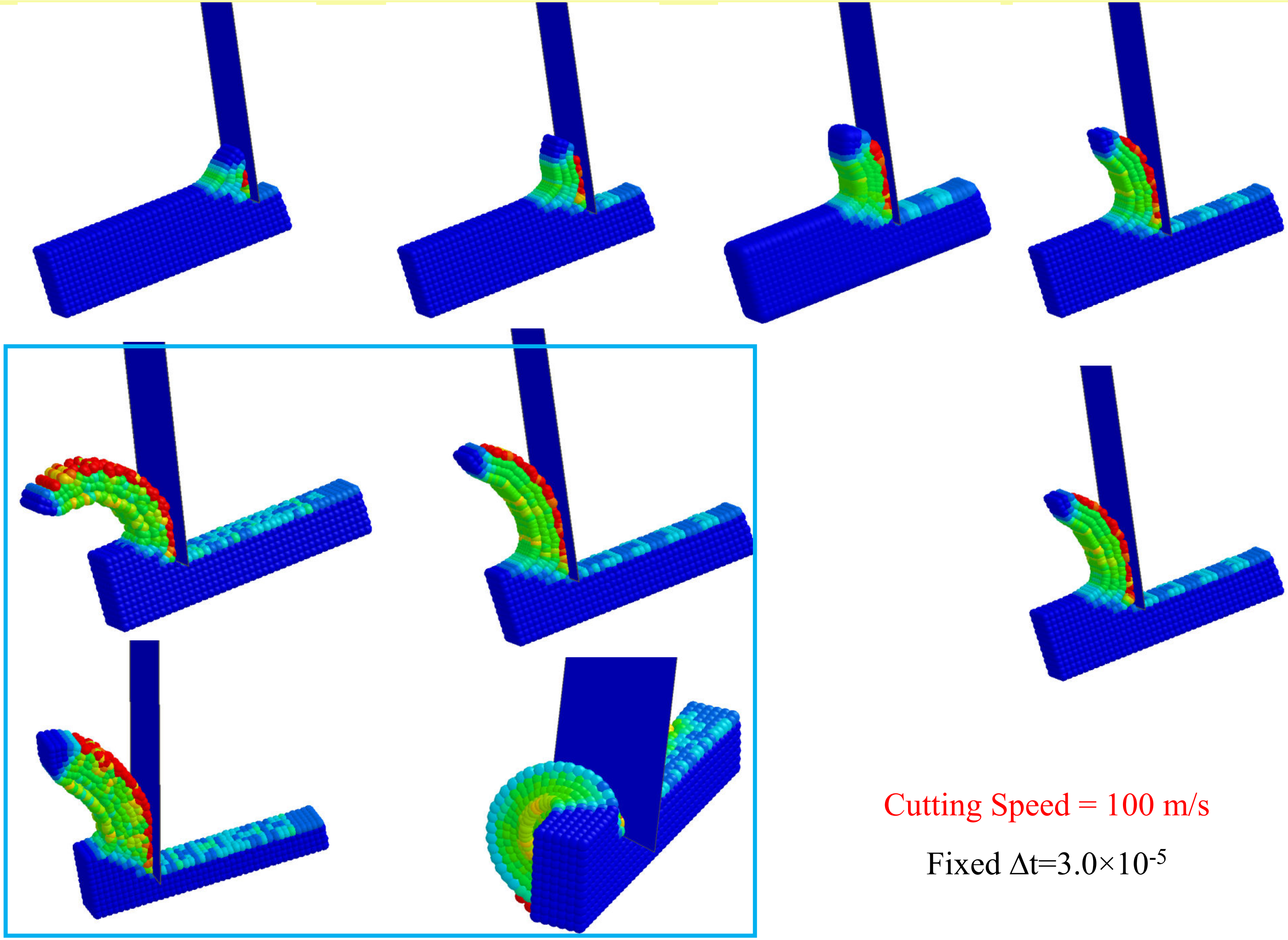

Cutting Speed = 100 m/s

Fixed $\Delta t=3.0\times10^{-5}$

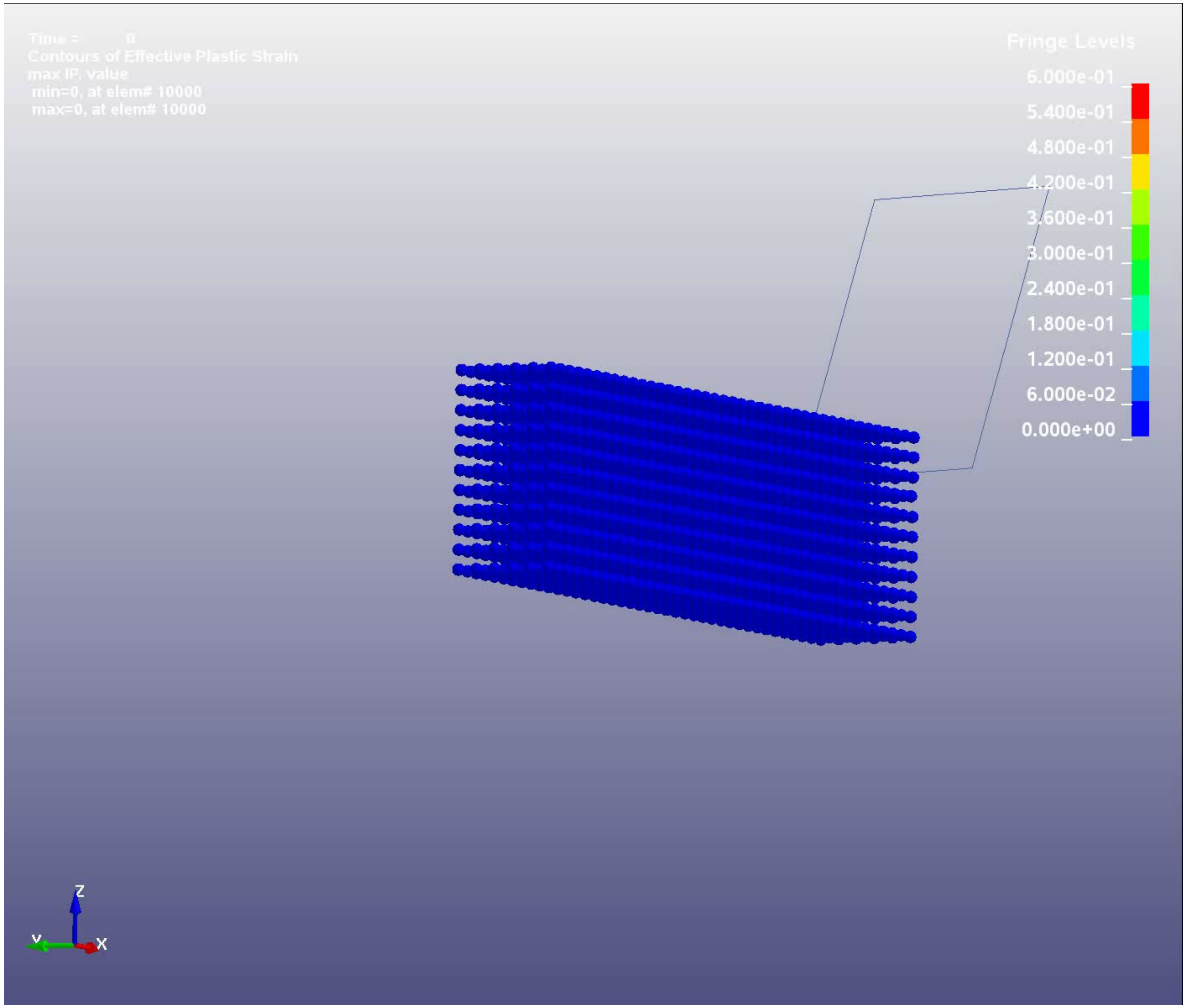
Time = 0
Contours of Effective Plastic Strain
max IP. value
min=0, at elem# 10000
max=0, at elem# 10000
Fringe Levels
6.000e-01
5.400e-01
4.800e-01
4.200e-01
3.600e-01
3.000e-01
2.400e-01
1.800e-01
1.200e-01
6.000e-02
0.000e+00
Z
Y
X

Metal shearing analysis

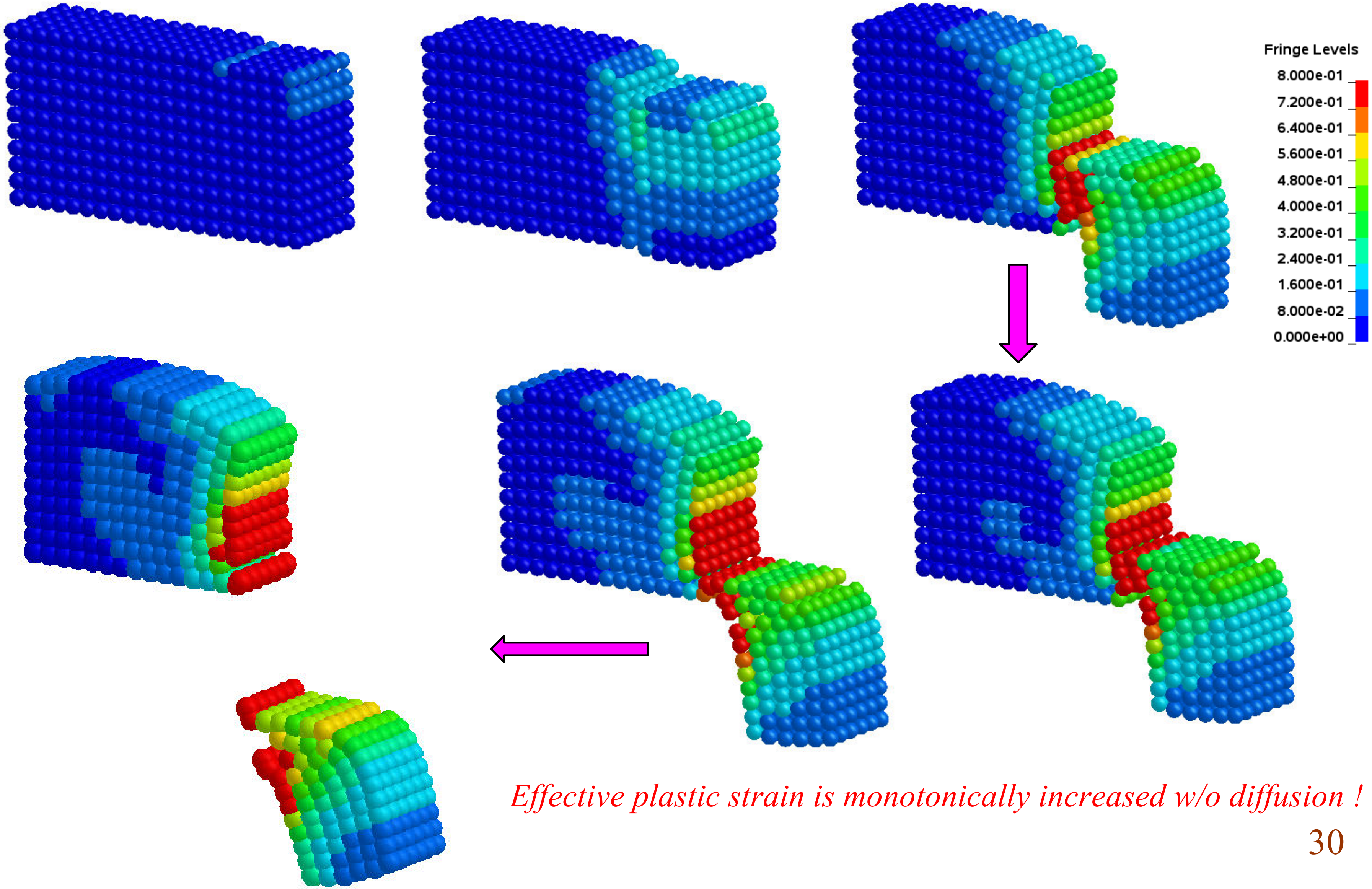

Effective plastic strain is monotonically increased w/o diffusion !

Keyword Input Format

*SECTION_SOLID_SPG

Card1	1	2	3	4	5	6	7	8
Variable	SECID	ELFORM	AET					
Type	I	47	I					
Default								

Card2	1	2	3	4	5	6	7	8
Variable	DX	DY	DZ	ISPLINE	KERNEL	LSCALE	SMSTEP	SWTIME
Type	F	F	F	I	I	F	I	F
Default	1.5	1.5	1.5	0	3		15	
Card3	1	2	3	4	5	6	7	8
Variable	IDAM	FS	STRETCH					
Type	I	F						
Default	0							

VARIABLE	DESCRIPTION
SECID	Section ID.
ELFORM	Element formulation options. Set to 47 to active SPG method.
DX, DY, DZ	Normalized dilation parameters of the kernel functions in X, Y and Z directions.
ISPLINE	Option for kernel functions. EQ.0: Cubic spline function (default). EQ.1: Quadratic spline function. EQ.2: Cubic spline function with circular shape.
KERNEL	Type of kernel approximation. EQ.0: updated Lagrangian kernel. EQ.1: Eulerian kernel. EQ.2: Semi-Lagrangian kernel. EQ.3: Pseudo-Lagrangian kernel.
LSCALE	Length scale for displacement regularization.
SMSTEP	Interval of time steps to conduct displacement regularization.
SWTIME	Time to switch from updated Lagrangian kernel to Eulerian kernel.
IDAM	Damage option. EQ.0: Continuum damage mechanics (default) EQ.1: Phenomenological strain damage EQ.2: Maximum principal strain damage
FS	Failure strain if IDAM=1; maximum principal strain if IDAM=2
STRETCH	Stretching parameter if IDAM=1

Conclusions and Future Plans

1. Smoothed Particle Galerkin (SPG) Method is implemented in LS-DYNA® and a SMP trial version is available.
2. Mathematical and numerical properties have been provided.
3. The method is able to handle severe deformation involving material failure for various solid applications.
4. The application to compressible fluids or fluid-type solids is currently excluded.
5. Official SMP and MPP versions will be released in this year.
6. The extension to adaptive FEM/EFG method will be considered.
7. The switch from FEM to SPG method for severe deformation analysis will be implemented.